



This is a repository copy of *Pervasive mimicry in flight behavior among aposematic butterflies*.

White Rose Research Online URL for this paper:

<https://eprints.whiterose.ac.uk/209671/>

Version: Published Version

Article:

Page, E. orcid.org/0000-0003-4381-1025, Queste, L.M. orcid.org/0000-0002-7402-8079, Rosser, N. et al. (6 more authors) (2024) Pervasive mimicry in flight behavior among aposematic butterflies. *Proceedings of the National Academy of Sciences*, 121 (11). ISSN 0027-8424

<https://doi.org/10.1073/pnas.2300886121>

Reuse

This article is distributed under the terms of the Creative Commons Attribution-NonCommercial-NoDerivs (CC BY-NC-ND) licence. This licence only allows you to download this work and share it with others as long as you credit the authors, but you can't change the article in any way or use it commercially. More information and the full terms of the licence here: <https://creativecommons.org/licenses/>

Takedown






If you consider content in White Rose Research Online to be in breach of UK law, please notify us by emailing eprints@whiterose.ac.uk including the URL of the record and the reason for the withdrawal request.



eprints@whiterose.ac.uk
<https://eprints.whiterose.ac.uk/>



Pervasive mimicry in flight behavior among aposematic butterflies

Edward Page^{a,1,2} , Lucie M. Queste^{a,b,2} , Neil Rosser^{a,c,2}, Patricio A. Salazar^{d,e} , Nicola J. Nadeau^d , James Mallet^c , Robert B. Srygley^{f,g}, W. Owen McMillan^f, and Kanchon K. Dasmahapatra^{a,1}

Edited by Marlene Zuk, University of Minnesota, St. Paul, MN; received February 14, 2023; accepted January 10, 2024

Flight was a key innovation in the adaptive radiation of insects. However, it is a complex trait influenced by a large number of interacting biotic and abiotic factors, making it difficult to unravel the evolutionary drivers. We investigate flight patterns in neotropical heliconiine butterflies, well known for mimicry of their aposematic wing color patterns. We quantify the flight patterns (wing beat frequency and wing angles) of 351 individuals representing 29 heliconiine and 9 ithomiine species belonging to ten color pattern mimicry groupings. For wing beat frequency and up wing angles, we show that heliconiine species group by color pattern mimicry affiliation. Convergence of down wing angles to mimicry groupings is less pronounced, indicating that distinct components of flight are under different selection pressures and constraints. The flight characteristics of the Tiger mimicry group are particularly divergent due to convergence with distantly related ithomiine species. Predator-driven selection for mimicry also explained variation in flight among subspecies, indicating that this convergence can occur over relatively short evolutionary timescales. Our results suggest that the flight convergence is driven by aposematic signaling rather than shared habitat between comimics. We demonstrate that behavioral mimicry can occur between lineages that have separated over evolutionary timescales ranging from <0.5 to 70 My.

parallel evolution | multitrait mimicry | wing beat frequency | *Heliconius* | Ithomiini

The evolution of powered flight likely played a key role in the adaptive radiations of insects (1), bats (2), and birds (3). Flight is a complex trait characterized by variation in wing beat frequency, flight speed, acceleration, maneuverability, stroke amplitude, and asymmetry, which may be produced by changes in wing shape and structure, musculature, and physiology (3). While much research has focused on understanding the aerodynamics (4) and origin (5) of flight, relatively little is known about the evolutionary pressures driving the diversification of flight behaviors within these groups (6, 7).

Factors affecting flight could include abiotic drivers associated with habitat such as air pressure (due to elevation) (8, 9), temperature (particularly important for ectotherms) (10), and the complexity of the habitat itself. Biotic drivers include species morphology (11), life history traits like migration behavior (12) and foraging needs (13) among others. These factors will likely interact in complex and sometimes antagonistic ways, potentially constraining the ability of selection to affect flight along any particular axis. For example, in some *Morpho* butterflies, males are found gliding in the canopy while females utilize flapping flight in the understory (14). The canopy-flying males have a higher wing aspect ratio (14), which is associated with increased aerodynamic efficiency and reduced energetic cost of flight (15). However, despite these energetic advantages, females in the same group use flapping flight because they are constrained by microhabitat, as they spend a significant amount of time flying in the understory searching for oviposition sites (14). Male *Morpho* butterflies also alter their flight behavior when conspecific butterflies are present and exhibit a different flight pattern depending on the sex of the individual with which they are interacting (16).

Flight behavior may also be influenced by predation. In diurnal Lepidoptera (butterflies and moths), predation pressure has led to the widespread evolution of mimetic aposematic wing color patterns. This mimicry among individuals from often unrelated species is commonly classified as either mutualistic (Müllerian mimicry), with multiple unpalatable taxa sharing similar warning patterns, or parasitic (Batesian mimicry), with palatable individuals gaining protection by mimicking unpalatable taxa (17–19). Although behaviors have been recognized as an important component of the mimetic signal, studies of mimicry often focus on single trait, static signals such as color pattern (20–22). However, multitrait mimicry is expected to create a more robust signal and may reduce the need for close mimicry of individual traits. Behavioral mimicry has been directly shown to provide protection from predators; for example, in Salticid spiders,

Significance

Predation drives evolutionary convergence in warning coloration and is also expected to promote behavioral resemblance between mimetic species. Using high frame rate video footage of neotropical mimetic butterflies, we show that butterflies belonging to the same color pattern mimicry group have also converged in flight behavior. Our results demonstrate that flight mimicry has evolved between species that separated recently as well as those that split over 70 Mya, and that this behavioral mimicry even matches color pattern variation found within species. Thus, we reveal pervasive behavioral mimicry across a very broad range of evolutionary timescales.

Author contributions: L.M.Q., N.R., and K.K.D. designed research; E.P., L.M.Q., N.R., P.S., and N.N. performed research; E.P., L.M.Q., and N.R. analyzed data; P.S. collected and provided additional samples; and E.P., L.M.Q., N.R., N.N., J.M., R.B.S., W.O.M., and K.K.D. wrote the paper.

The authors declare no competing interest.

This article is a PNAS Direct Submission.

Copyright © 2024 the Author(s). Published by PNAS. This article is distributed under [Creative Commons Attribution-NonCommercial-NoDerivatives License 4.0 \(CC BY-NC-ND\)](https://creativecommons.org/licenses/by-nc-nd/4.0/).

¹To whom correspondence may be addressed. Email: ejp548@york.ac.uk or kanchon.dasmahapatra@york.ac.uk.

²E.P., L.M.Q., and N.R. contributed equally to this work.

This article contains supporting information online at <https://www.pnas.org/lookup/suppl/doi:10.1073/pnas.2300886121/-/DCSupplemental>.

Published February 26, 2024.

where ant-mimicking spiders are significantly less likely to be predated than con- or heterospecific non-ant-mimicking individuals (23).

There are some limited examples of flight mimicry in insects. For example, in the butterfly *Papilio polytes*, mimetic female morphs show stronger similarities in flight to their putative model species than nonmimetic males and palatable controls (24). Bee and wasp-mimicking sesiid moths have also been shown to fly more similarly to their respective models than to nonmimetic sesiids (25). Flight mimicry has been demonstrated between two comimetic species pairs of *Heliconius* butterflies (26). However, these studies are limited both in their taxonomic scope and evolutionary time frame, and comprehensive investigation of the evolution of multitrait mimicry is lacking.

Color pattern mimicry is particularly common in certain butterflies, such as the well-studied neotropical heliconiine butterflies (27). This group of ~77 species (28) display conspicuous warning color patterns associated with unpalatability to potential predators, usually diurnal insectivorous birds (29–31). Near identical color patterns have evolved in multiple species, resulting in the formation of characteristic mimicry rings (32, 33). These mimicry rings usually comprise other heliconiine butterflies but may also include more distantly related butterfly taxa and even day-flying moth species (32). The orange/yellow/brown “Tiger” mimicry ring in particular is dominated by species belonging to another distantly related distinct aposematic butterfly tribe, the Ithomiini (34), which have been suggested to be the primary unpalatable models (35). The Ithomiini are a diverse tribe of over 350 species, most belonging to a variety of transparent mimicry groupings (34).

There is tantalizing evidence that mimicry in *Heliconius* butterflies extends beyond color patterns to other traits. In addition to the limited evidence of flight mimicry, studies of wing shape have also found convergence within mimicry groups in a few *Heliconius* species (36–39). Convergence in wing shape can potentially increase both visual mimicry, when butterflies are static (for example, during basking and roosting behavior), and behavioral mimicry by influencing flight aerodynamics. Although there are some habitat differences between mimicry rings, species belonging to multiple mimicry rings commonly co-occur and also overlap in flight height (32). The Heliconiini are also a very ecologically diverse clade, with species ranging widely across the neotropics (40), and found across elevational gradients and different habitat types. Various traits including wing shape variation have been attributed to differences in altitude (41), microhabitat (42), and flight strata (43). Therefore, the scale and importance of multitrait mimicry in this textbook system of convergent evolution is unknown.

In this study, we characterize the flight of 29 heliconiine and 9 ithomiine species. After controlling for phylogenetic relatedness, we test for the effect of multiple biotic and abiotic factors (mimicry, habitat, location, temperature, and morphology) on flight behavior in a system exhibiting Müllerian mimicry of wing color patterns between taxa that diverged as recently as 0.5 Mya to as long as 70 Mya (44, 45).

Results

Wing beat frequency (WBF) was measured for 351 individuals (199 males and 152 females) from 29 heliconiine (44 subspecies) and 9 ithomiine species belonging to 10 mimicry rings. Wing angle estimates were obtained for a subset of 240 of the heliconiine individuals from all the species, excluding *Dione juno*, and from 26 ithomiine individuals representing all 9 species. WBF and up

wing angles are correlated with one another ($r = 0.56$, $P < 0.0001$), but there is no correlation between WBF and down wing angles ($r = 0.044$, $P = 0.49$) or between the two wing angles ($r = -0.12$, $P = 0.059$) (*SI Appendix*, Fig. S1) (Fig. 1).

Individual-Based Models. Flight in butterflies is often affected by wing dimensions and body mass. Using the four species for which we had morphology measures of the individuals whose flight was measured, we tested the extent to which variation in WBF and wing angles is caused by morphological (wing aspect ratio, wing area, forewing length, fresh body mass, and wing loading) or behavioral differences between taxa. Other than a significant negative effect of forewing length on WBF explaining 3% of the variance, we did not detect effects of any of the morphology variables on WBF or either wing angle, and models excluding the morphology variables were a better statistical fit to the data (*SI Appendix*, Fig. S2). It is possible that with larger sample sizes additional subtle effects of the other morphology measures on flight may be found.

Relationship between Mimicry Affiliation and Wing Beat Frequency. Among the Heliconiini, the Tiger group has the lowest mean WBF (9.5 ± 1.2 Hz), and after controlling for phylogenetic nonindependence, its members have a significantly slower WBF than most other mimicry groups. The members of the orange mimicry group have a mean WBF significantly higher (14.3 ± 2.4 Hz) than most other mimicry groups (Table 1A and Fig. 2). Although most members of the heliconiine Tiger mimicry ring are closely related to one another (Fig. 2), the basal comimetic *Eueides isabella* also shares this slow WBF. In addition, *Heliconius elevatus*, the only dennis-rayed species among the group of closely related Tiger species, has a faster WBF, matching that of the other dennis-rayed species (Fig. 2). The distantly related ithomiine members of the Tiger mimicry ring were found to have a WBF of 9.6 ± 1.4 Hz, similar to that of the heliconiine Tigers, while the transparent ithomiini have a higher WBF of 12.3 ± 1.2 Hz. Our models indicate that WBF is significantly different in the majority of pairwise comparisons between mimicry groups demonstrating that WBF mimicry is widespread across the Heliconiini (Table 1A). There was no significant effect of habitat in any of the models we ran (Dataset S2–LRT applied to random effect d_{pp} ; a significant effect would indicate that species which share habitats have similar WBFs). We therefore excluded this term from the final models.

In addition to the association with color pattern mimicry rings, WBF was significantly higher at lower temperatures and in butterflies with shorter forewings. Butterflies in Peru had faster WBFs than those in Panama (Dataset S2 and *SI Appendix*, Fig. S3). This effect is especially clear when the WBF of the six species found in both Peru and Panama are compared, with all six showing higher WBFs in Peru (*SI Appendix*, Fig. S3). We also detected significant individual and species effects (Dataset S2). We did not detect any significant effect of total wing area, body mass, wing aspect ratio, wing loading, or sex differences on WBF (Dataset S2).

Relationship between Mimicry Affiliation and Wing Angles. Mirroring the WBF results, aside from transparent ithomiine butterflies ($40 \pm 7^\circ$), the heliconiine members of the Tiger mimicry ring have the most distinct mean up wing angle ($55 \pm 12^\circ$) which, after taking into account phylogenetic nonindependence, is significantly narrower than the angles of all other mimicry rings (Table 1A, Fig. 2, and *SI Appendix*, Fig. S4) and very similar to that of the Tiger ithomiine butterflies ($53 \pm 13^\circ$). Significant differences

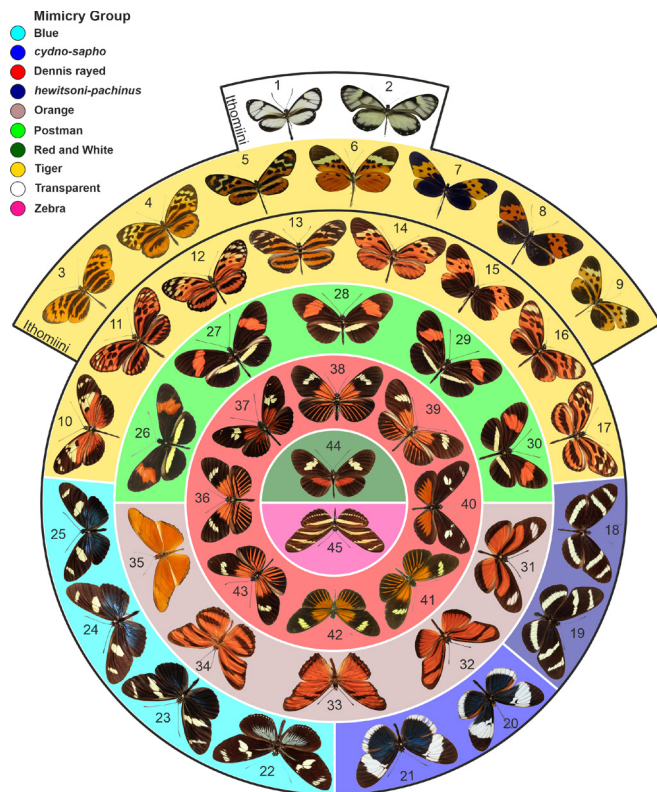


Fig. 1. Diversity and convergence of wing patterns among the heliconiine and ithomiine taxa whose flight patterns have been measured. Background color indicates the 10 mimicry groups. Transparent (ithomiine) 1: *Ithomia salapia travella*, 2: *G. zavaleta*; Tiger (Ithomiine) 3: *Melinaea marseus phasiana*, 4: *Tithorea harmonia*, 5: *Mechanitis polymnia*, 6: *Melinaea menophilus zaneka*, 7: *Mechanitis messenoides deceptus*, 8: *Melinaea mothone mothone*, 9: *Hypothyris anastasia honesta*; Tiger (Heliconiine) 10: *Heliconius ismenius bouletti*, 11: *H. p. butleri*, 12: *Heliconius hecale felix*, 13: *Eueides isabella nicaraguensis*, 14: *H. pardalinus sergestus*, 15: *Heliconius numata bicoloratus*, 16: *Heliconius numata aurora*, 17: *Heliconius ethilla aerotome*; hewitsoni-pachinus 18: *H. pachinus*, 19: *Heliconius hewitsoni*; cydno-sapho 20: *Heliconius cydno chioneus*, 21: *Heliconius sapho sapho*; Blue 22: *Heliconius doris viridis blue*, 23: *Heliconius wallacei flavascens*, 24: *Heliconius leucadia pseudorhea*, 25: *Heliconius sara sara*, Postman 26: *Heliconius timareta thelxinoe*, 27: *Heliconius melpomene rosina*, 28: *H. e. favorinus*, 29: *Heliconius erato demophoon*, 30: *Heliconius melpomene amaryllis*; Orange 31: *Eueides lybia olympia*, 32: *Eueides aliphera aliphera*, 33: *Dione juno juno*, 34: *Dryadula phaetusa*, 35: *D. iulia*; Dennis rayed 36: *Heliconius elevatus pseudocupideneus*, 37: *Heliconius burneyi huebneri*, 38: *Heliconius aede cupidensis*, 39: *Heliconius melpomene aglaope*, 40: *Heliconius doris viridis*, 41: *Heliconius eratosignis*, 42: *Heliconius demeter joroni*, 43: *H. e. emma*; Red and white 44: *H. himera*; Zebra 45: *H. charithonia*. Butterflies images are from the Neukirchen Collection, McGuire Centre, Florida; <https://www.butterfliesofamerica.com/> (Andrew Warren); <http://www.sangay.eu/esdex.php/> (Jean-Claude Petit).

in up wing angle were not observed between any of the other mimicry rings other than Zebra, which is only represented by a single taxon (Table 1B and Fig. 2). Up wing angles were found to be larger at lower temperatures (Dataset S2). In our models, we do not detect any effect of location, morphology, or sex on up wing angle (Dataset S2).

While there is no mimicry group that has a very distinct down wing angle, our models demonstrate that there are small but significant differences between some mimicry groups (Table 1B and SI Appendix, Fig. S5). Unlike WBF and up wing angles, the down wing angle of the heliconiine Tiger mimicry ring is not very distinct. Down wing angle was also affected by multiple morphology measures; the angles were found to be larger with smaller aspect ratio, larger wing area, and lower wing loading. No effect of location, sex, or body mass on down wing angle was detected.

We also detected significant individual and species effects on up wing angle and a significant effect of individual on down wing angle (Dataset S2). As with WBF, we detected no significant effect of habitat (d_{spp}) in any of the wing angle models (Dataset S2–LRT applied to random effect d_{spp}) and therefore excluded this term from the final models.

Wing Beat Frequency Mimicry at the Intraspecific Level.

Comparing comimetic parapatric subspecies of Peruvian *Heliconius melpomene* and *Heliconius erato*, butterflies of both species in the postman mimicry group (*Heliconius melpomene amaryllis* and *Heliconius erato favorinus*) had a significantly higher WBF compared to the dennis-rayed subspecies (*H. melpomene aglaope* and *Heliconius erato emma*) ($B = 0.84$, $SE = 0.38$, $t = 2.2$, $P = 0.049$). There was no significant difference in WBF between the species ($B = 0.35$, $SE = 0.43$, $t = 0.81$, $P = 0.43$). No significant differences were found in wing angles between mimicry groups (up angles: $B = 7.39$, $SE = 9.1$, $t = 0.81$, $P = 0.44$; down angles: $B = -4.36$, $SE = 5.64$, $t = -0.77$, $P = 0.47$) or species (up angles: $B = 11.47$, $SE = 9.83$, $t = 1.17$, $P = 0.27$; down angles: $B = -4.86$, $SE = 6.471$, $t = -0.751$, $P = 0.481$).

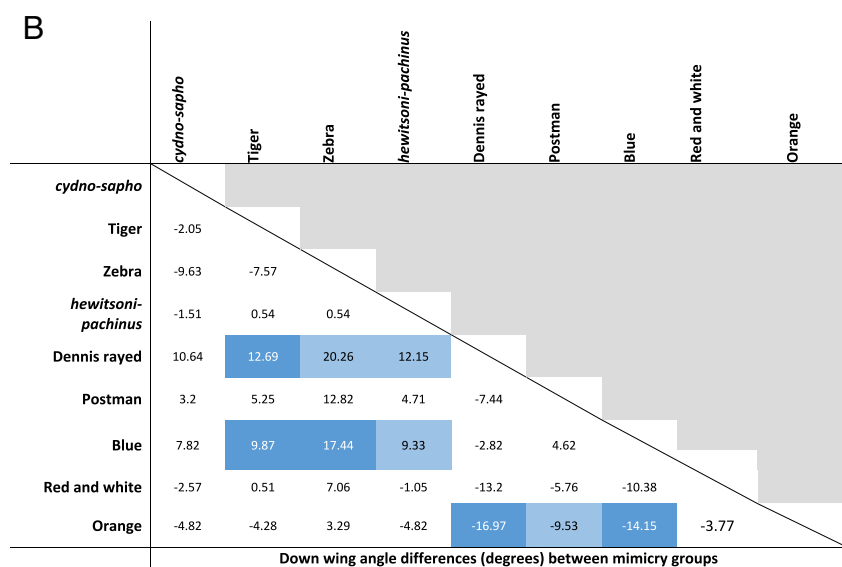
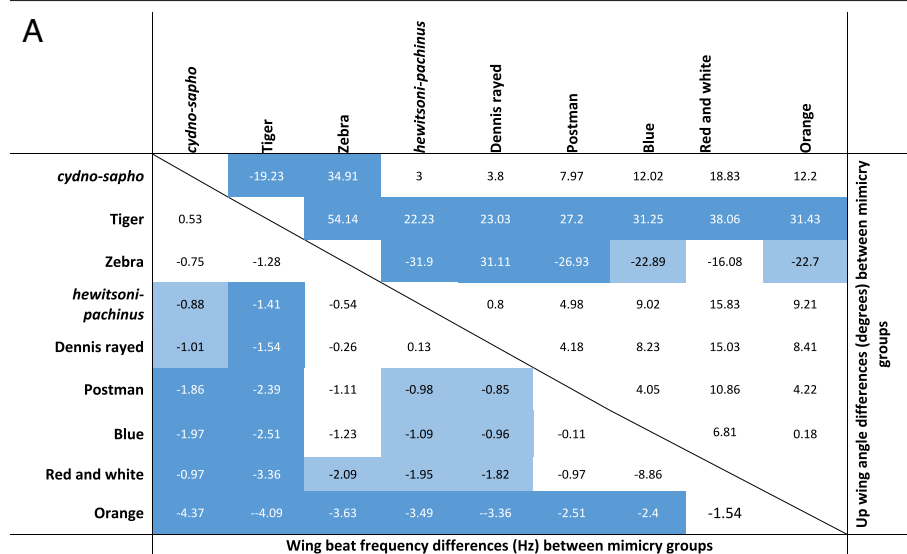
Does Shared Habitat or Mimicry Have a Stronger Effect on Flight Convergence?

If flight convergence is more influenced by selection caused by predation pressure than selection due to the habitat, then the correlation between flight similarity and phylogenetic relatedness is expected to be weaker among mimetic co-occurring species compared to nonmimetic co-occurring species. Accordingly, we find significant positive correlations between phylogenetic distance and differences in both WBF ($r = 0.47$, $P = 0.00002$) and up wing angle ($r = 0.25$, $P = 0.01$) among co-occurring nonmimetic species. In contrast, among the co-occurring mimetic species there is no correlation between phylogenetic distance and differences in either WBF ($r = 0.22$, $P = 0.89$) or up wing angle ($r = 0.03$, $P = 0.56$). We did not find significant correlations between differences in down wing angles and phylogenetic distance in either group. Therefore, convergence in WBF and up wing angle is strongly associated with color pattern mimicry rather than shared habitat, a finding consistent with the absence of habitat effects in our phylogenetic linear mixed models (PLMMs). The frequency distribution of correlation coefficients from the 20,000 randomized trees used to derive P -values is shown in supplementary SI Appendix, Fig. S6.

Discussion

Evidence for mimetic convergence is widespread in many taxa (for example, refs. 46 and 47). Mimicry can be a highly complex trait that extends to morphological features (39), chemical signals (48), and behavior (26). Multitrait mimicry could evolve to produce a more complex and robust mimetic signal (26) and to supplement imperfect morphological mimicry of individual traits (49). Here, we demonstrate that multiple factors affect flight behavior in heliconiine butterflies, but that the association between color pattern mimicry affiliation and convergence in flight (WBF and up wing angles) is particularly strong (Fig. 2). Our data indicate that convergence of flight behavior mainly results from predator-driven selection due to mimicry rather than shared habitat of comimics. Evidence of flight pattern mimicry is found between species spanning the entire Heliconiini tribe and is even present between the Tiger-patterned heliconiines and their distantly related Ithomiine mimetic models. Significant differences in WBF were also found between the subspecies of individual species (Fig. 3), and these differences were shared between comimetic subspecies of different

Table 1. Pairwise differences in flight behavior between heliconiine mimicry groups



Models include two principal components as covariates capturing >99% of the variation in three morphology measures (forewing length, total wing area, and aspect ratio). (A) Figures show the difference in wing beat frequency (bottom left triangle) and up wing angle (top right triangle) and in (B) the difference in down wing angle, between the left mimicry group and top mimicry group. To obtain the difference in trait value between all pairwise comparisons of mimicry rings, each mimicry ring was set in turn as the intercept in the PLMMs. Significance values are indicated by color: $P < 0.05$ (light blue), $P < 0.01$ (dark blue). Note that the Zebra and red and white mimicry groups are only represented by single taxa.

species, indicating that evolution of flight mimicry can occur over relatively short evolutionary time scales. The patterns of flight mimicry we show are clear even though we were unable to properly control for morphology of the filmed individuals and instead used species average values for these variables. On the basis of our individual data, these morphology variables seem to have relatively little influence, at most explaining 3% of the variation in flight parameters.

Overall, we demonstrate that behavioral mimicry is present across the entire Heliconiini tribe and beyond and therefore that complex multitrait mimicry is common in this aposematic group of butterflies. The convergent effects of flight mimicry are particularly clear in cases like *H. elevatus*, a dennis-rayed species in a clade dominated by Tiger-patterned species, and *E. isabella* the only sampled Tiger in an otherwise orange clade (Fig. 1). In both cases, the species in question show WBF and up wing angles similar to their more distantly related comimics than to their closest relatives. More generally, the many members of the dennis-rayed mimicry

ring are phylogenetically widely distributed yet show strongly convergent WBF and wing angles.

Among the Heliconiini, the mimicry ring with the most distinct flight pattern is the Tiger group, which has both the lowest WBF and the narrowest up wing angle. The convergence in WBF between heliconiine and ithomiine members of the Tiger mimicry ring, which diverged from one another ~70 Mya (45), is striking. The Ithomiini are thought to be the main mimetic models in the Tiger mimicry ring (35) as it is dominated by a large number of chemically defended ithomiine species (35, 50) belonging mainly to the *Melinaea*, *Hypothyris*, *Mechanitis*, and *Tithorea* genera (51). The Ithomiini have very different ecologies to the Heliconiini, for example, in host plant usage (52), defensive toxins (53), brain composition (54, 55), and pheromones (56, 57). Our limited sampling of transparent ithomiine species suggests that while transparent and Tiger ithomiine species appear to have distinct WBF, the narrow up wing angles seem characteristic of the Ithomiini regardless of mimicry affiliation. Taken together, the very distinct flight patterns

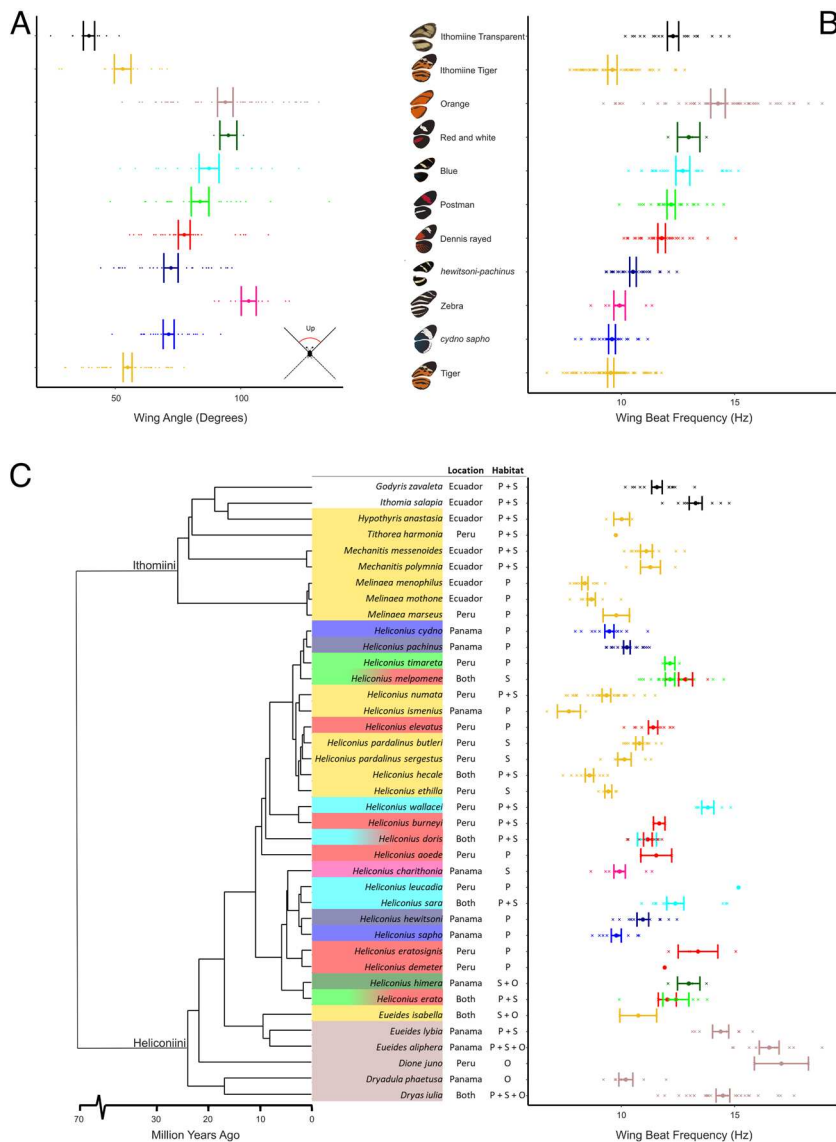


Fig. 2. Variation in flight behavior among mimicry groups. The (A) mean up wing angle (see *Inset* diagram) and (B) mean wing beat frequency ± 1 SE for each mimicry group. Data points are the measurements made from all the recorded individuals for each taxon. (C) Phylogenetic relationships among the species used in the analyses of wing beat frequency. Mean wing beat frequency ± 1 SE for each taxon is shown, together with data points representing measurements made from all individuals. Species names and data points are colored by mimicry ring. Species with subspecies belonging to multiple mimicry rings are shown with multicolored names. For habitat types, P = Primary/tall forest, S = Secondary/degraded forest, O = Open forest or field environments.

of the heliconiine Tiger mimicry ring suggest that its members have converged on the flight patterns exhibited by the Tiger Ithomiini. Subtle fine-scale mimicry may also be present between similarly patterned species within the Tiger mimicry group, with flight patterns among the heliconiine Tigers mirroring those of their specific ithomiine comimics. Better sampling of transparent ithomiine taxa may also reveal pervasive flight mimicry within this large and diverse group similar to our findings within the Heliconiini.

Among the other factors we found to affect flight patterns, the effect of sampling location is likely a consequence of the Peruvian sampling sites and flight cages being situated at an elevation ~ 350 m higher than those in Panama, although we cannot rule out other factors related to cage location such as the extent of exposure to the sun. Similar effects of elevation have been observed in migratory birds (58). Higher elevation correlates with a number of flight relevant environmental variables [lower air density, temperature and oxygen levels (59)], and we find that Peruvian taxa had significantly higher WBF than Panamanian species (*SI Appendix, Fig. S3*). Elevation has also been shown to correlate with wing

shape in *Heliconius* (41), and this may in turn also influence flight behavior (60).

Habitat complexity is expected to impose different constraints upon flight. For example, species such as *Eueides aliphera*, which is typically found in forest clearings, are likely to experience a very different flight environment to *Heliconius aoede*, which is found in closed forest (40).

However, our PLMMs and tests based on comparing phylogenetic signals in flight measures between co-occurring mimetic and nonmimetic species both indicate that convergence in WBF and up wing angles among species is more strongly associated with species' color pattern mimicry affiliation than their habitat. They suggest that convergence in these flight characters is a consequence of selection pressure from predators promoting behavioral mimicry rather than due to shared habitat. In contrast, several lines of evidence suggest that the selective pressures acting on down wing angles may be different to those acting on WBF and up wing angles. First, unlike the other flight characters, we find that down wing angles are correlated with multiple wing and other flight-related

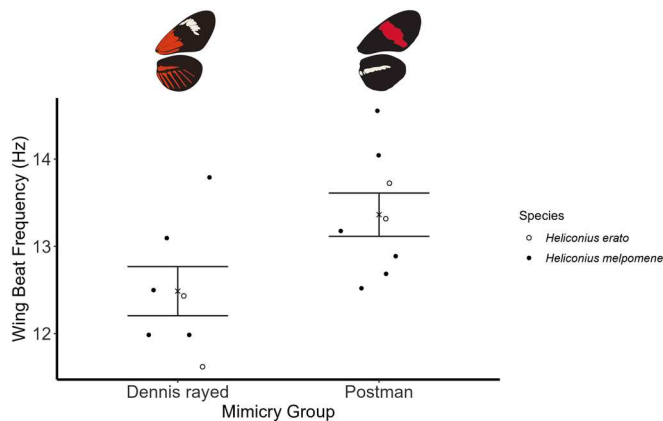


Fig. 3. Convergence in wing beat frequency among comimetic subspecies of *Heliconius erato* and *Heliconius melpomene*. Butterflies in the Peruvian Postman mimiry group (*H. e. favorinus* and *H. m. amaryllis*) have a significantly higher wing beat frequency ($B = 0.84$, $SE = 0.38$, $t = 2.2$, $P = 0.049$) compared to Peruvian Dennis-rayed butterflies (*H. e. emma* and *H. melpomene aglaope*). Wing beat frequency is not significantly different between species ($B = 0.35$, $SE = 0.43$, $t = 0.81$, $P = 0.43$). The mean wing beat frequency (± 1 SE) is shown for each mimiry group. Each stack of points represents multiple measurements from the same individual.

morphologies (Dataset S2). Second, the results of the PLMMs show that relatively few mimiry groups have different down wing angles, and that the Tiger mimiry group with its very distinct WBF and up angles is not distinctive in its down wing angle (Table 1). Third, unlike for WBF and up wing angles, co-occurring mimetic and nonmimetic taxa have similar nonsignificant phylogenetic signals in their down wing angles (SI Appendix, Fig. S6). These all suggest that down wing angles respond differently to selection exerted by predators and may be indicative of greater aerodynamic constraint on this trait. Fuller characterization of flight may provide stronger evidence of whether different components of flight are evolving under different selection pressures.

Flight mimicry between comimetic Peruvian subspecies of *H. erato* and *H. melpomene* is remarkable as these parapatric subspecies are young [*H. e. emma* and *H. e. favorinus* are estimated to have diverged 330 to 500 thousand years ago (44)]. This suggests that in this system even complex behavioral mimicry can evolve rapidly, although the generality of this across other subspecies, or indeed across the rest of the Heliconiini remains untested. Rapid evolution of different intraspecific color pattern variants in *Heliconius* is a consequence of the phenotypes being controlled by a small number of major effect loci, each associated with multiple cis-regulatory modules (61, 62). Shuffling of these modules through recombination between lineages can rapidly generate new phenotypes, and similar mechanisms may also allow rapid diversification of flight patterns. In both species, the subspecies are genetically very similar, with only a few narrow regions of genetic differentiation distinguishing each subspecies (62, 63). Most of these regions are associated with known color pattern loci, raising the possibility that loci controlling flight may be genetically linked to these color pattern loci. Such linkage could potentially provide another route to flight mimicry, allowing particular flight characteristics to be associated with certain color pattern alleles. In support of this hypothesis, there is close correspondence between quantitative trait loci controlling colour pattern, WBF and wing shape in crosses between the dennis-rayed *H. elevatus* and Tiger-patterned *H. pardalinus* (64). The generality of this finding is unknown, and it remains to be discovered whether the genetic architecture of flight patterns mirrors that of color patterns, with mimicry between closely related taxa resulting from collateral evolution via hybridization, and extensive parallel evolution occurring between more distantly related species.

Across the Heliconiini and beyond, mimicry group is a key determinant of flight behavior and explains more variation in the trait than factors typically associated with flight behavior, such as wing size (65, 66). This serves as quantitative evidence of behavioral mimicry across a large, phenotypically and phylogenetically diverse group. Flight behavior has converged between taxa that evolved across a broad range of evolutionary timescales, raising important questions about the genetic mechanisms behind the convergent evolution of this highly complex trait.

Materials and Methods

Filming Butterflies. Wild-caught heliconiine butterflies (Fig. 1 and Dataset S1) were housed in outdoor insectaries in Tarapoto, Peru (15 species), Gamboa, Panama (15 species, including 6 also filmed in Peru), and IKIAM, Ecuador (2 species). Additionally, a few ithomiine species belonging to the Tiger and transparent mimiry groupings (Fig. 1 and Dataset S1) were also kept in Peru (2 species) and IKIAM, Ecuador (5 species). When individuals were collected at locations away from the filming sites, they were allowed to acclimatize to local conditions for at least 3 to 5 d prior to filming. For a few taxa (Dataset S1), the individuals used were captive-bred [maintained as detailed in Rosser et al. (67)] including the non-Panamanian species *Heliconius himera*, which was filmed in Panama. Butterflies were filmed flying freely in large outdoor flight cages [Panama: 1.5 m (W) \times 9 m (L) \times 2.5 m (H); Peru: 2.5 m (W) \times 5 m (L) \times 2 m (H); Ecuador: 2 m (W) \times 13 m (L) \times 2.2 m (H)] using GoPro HERO Black cameras at 239.7 frames per second and 720p resolution. Only individuals with intact or slightly damaged wings were filmed. Butterflies were introduced into the flight cages at least 15 min prior to filming. Individuals were generally left undisturbed but were occasionally agitated to induce flying. In these cases, measurements were not taken until the butterfly had returned to normal, undisturbed flight. Butterflies were filmed during the active hours of the day, between 08:30 and 17:00. Air temperature (varying between 19.6 and 36.5 °C) and weather conditions were recorded at the time of each flight, though sustained flight only occurred in sunny or partly overcast conditions.

Wing Beat Frequency and Wing Angle Measurements. Videos were analyzed in slow motion using GoPro Studio 2.5.9.2658. Flight sequences in which an individual was flying straight and level for at least five wing beats were selected to measure wing beat frequency (WBF). WBF was measured by counting the number of complete wing beats and the corresponding number of video frames which gives the flight time. Five WBF measurements were taken per individual from separate flight sequences. Where possible, these flight measurements were taken for five males and five females of each taxon (Dataset S1). The same flight sequences were also used to measure the angle made between the two wings at the peak upstroke and downstroke, which we refer to as up and down wing angles (Fig. 2A). This measure is related to stroke amplitude (the maximum and minimum elevation of the wing relative to the horizon) used in earlier work (68). To minimize parallax error, video frames in which the butterfly was level with and in front of the camera, and which showed the upper and lower extremes of the wing beat, were collected. Up and down wing angles (Fig. 2A) were measured from these images using ImageJ (69), with measurements taken from the clearly defined leading edge of the forewing. Where possible, five measurements for both the up and down angle were taken per individual. Video frames appropriate for measuring wing angle could not be obtained for *D. juno*.

Explanatory Variables. Previous studies (32, 40, 70) have classified species of Heliconiini as belonging in one of nine mimiry groups (dennis-rayed, postman, zebra, blue, *cydno-sapho*, *hewitsoni-pachinus*, orange, Tiger, red and white; Fig. 1) based on visual similarities and co-occurrence. These mimiry classifications are widely accepted among *Heliconius* biologists, and while they are mostly intuitive, could be seen as subjective. Therefore we used image analysis of wings to check these traditionally accepted mimiry groupings (SI Appendix, Fig. S7). Barring a few small discrepancies (discussed in SI Appendix), this analysis upheld the traditional mimiry groups. Therefore, each of our 34 taxa was placed in one of nine of these mimiry groups to allow the effect of mimiry ring membership on flight to be tested. We note that we only have data from single representatives of the zebra, and red and white groups, *Heliconius charithonia* and *H. himera* respectively. The ithomiine taxa we measured mainly belonged to

the Tiger group, together with two species from the large and diverse transparent mimicry group (Fig. 1).

Habitat complexity may affect flight patterns due to microclimate buffering (41) or due to habitat specific behavior (71). We assigned taxa as being present in one or more of three habitat types along an environmental gradient ranging from open habitat (scrub, field, semiagricultural), through secondary/degraded/edge forest, to primary forest (40, 72). This categorization was based on data reported in previous studies (43, 72, 73). In addition, we classified taxa biogeographically. For Peru, taxa were described as flying in the Upper Huallaga/Rio Mayo valley and/or in the Cordillera Escalera and/or in adjacent the Amazon lowlands regions. For Panama, we assigned taxa as being present in the Pacific and/or the central cordillera and/or the Caribbean.

Flight in butterflies is often affected by wing dimensions and body mass (74). To test the extent to which variation in WBF and wing angles is caused by morphological or behavioral differences between taxa, for four species (*Dryas iulia*, *Heliconius numata*, *Godyris zavaleta*, and *Ithomia salapia*), we measured wing aspect ratio, wing area (cm²), forewing length (cm), fresh body mass (g), and wing loading (N/cm²) of the individuals that were filmed. Body mass was measured immediately after the collection of flight data. The other parameters were measured from wing images using ImageJ (69). For all other, taxa we were unable to measure the wings of the individuals whose flight was assessed since either the wings were sampled destructively for another experiment, or because the wings had sustained additional damage after filming. Therefore, we obtained species average estimates of wing measurements from our existing butterfly collections. For most of these taxa, data were obtained from at least five individuals from both sexes. Fresh body mass measures were collected for 53% of heliconiine taxa (Dataset S1) allowing estimation of wing loading.

Air temperature and sex of individuals may also affect flight patterns and were also included in our statistical models, as was location (Peru/Panama).

To account for the phylogenetic nonindependence of the taxa, we used a previously published time-calibrated Bayesian phylogeny of the Heliconiini tribe with outgroups, estimated using 20 nuclear and 2 mitochondrial markers (28). Where we had flight data for a subspecies not represented in this phylogeny, we assigned the phylogenetic position and branch length of the most closely related taxon based on other studies (75, 76); for example, *H. cydno chioneus* was assigned to *H. cydno cordula* (Dataset S1). In cases where we had data from two subspecies within particular species (*H. doris*, *H. erato*, and *H. melpomene* from Peru), one of which was not represented in the published phylogeny, these were assigned conservatively as sisters with branch lengths of the most closely related pair of taxa (*H. pacheus/H. cydno*). Phylogenetic data was also missing for *Heliconius pardalinus sergestus*, which has been shown to be a divergent lineage rendering *H. pardalinus* paraphyletic (67). We therefore grafted the whole genome phylogeny (67) for this clade [*H. hecale*, (*H. p. sergestus*, (*Heliconius pardalinus butleri*, *H. elevatus*))] on to the multilocus phylogeny, with the branch lengths scaled using the species in common, *H. ethilla*.

Individual-Level Models. We used the data for the four species where we had morphology measures (wing aspect ratio, wing area, forewing length, fresh body mass, and wing loading measurements) of the individuals whose flight was measured to test the extent to which variation in WBF and wing angles is caused by morphological or behavioral differences between taxa. The dataset comprised *D. iulia* (WBF n = 10, wing angle n = 6), *H. numata* (WBF n = 10, wing angle n = 5), *G. zavaleta* (WBF n = 14, wing angle n = 6), and *I. salapia* (WBF n = 10, wing angle n = 5), all filmed in Ecuador. To understand the individual effect of each of these morphology variables, separate general linear models were fit including a species-morphology interaction, together with sex and temperature. These models were compared to simpler models with no morphology variable.

Phylogenetic Models. We analyzed wing beat frequency and wing angle of the heliconiine butterflies using PLMMs (77, 78) structured as follows:

$$Y_i = a + mimicry_i + temp_i + morphology_i + sex_i + site_i + a_{ssp[i]} + b_{ssp[i]} + c_{ssp[i]} + d_{ssp[i]} + e_i,$$

where $a \sim \text{Gaussian}(0, \sigma_a^2 I_n)$; $b \sim \text{Gaussian}(0, \sigma_b^2 V_n)$; $c \sim \text{Gaussian}(0, \sigma_c^2 I_n)$; $d \sim \text{Gaussian}(0, \sigma_d^2 V_n)$;

Y is the WBF, up wing angle or down wing angle for observation i in the dataset. The intercept a estimates the overall average value of Y across all observations, and e_i captures the residual variance. The fixed categorical effects *mimicry*, *sex*, and *site* denote the mimicry ring, sex, and the filming location. *temp* is a continuous fixed effect corresponding to temperature at the time of the observation. *morphology* is a continuous fixed effect corresponding to the species' average wing aspect ratio, wing area, forewing length, fresh body mass, or wing loading. To understand the individual effect of each of these variables, separate models were first fit including single *morphology* variables. Since these *morphology* measures may act in concert yet many of them are correlated, additionally separate models were fit using principal components covering >99% of the variation in these measures. Random variable a_{ssp} gives the differences in mean Y of different butterfly species, which are assumed to be drawn independently from a Gaussian distribution with mean 0 and variance σ_a^2 . Random variable b_{ssp} accounts for the phylogenetic relatedness among taxa. Specifically, b_{ssp} gives the differences in mean Y of different butterflies, but the differences between species are assumed to be drawn from a Gaussian distribution with covariance matrix $\sigma_b^2 V_n$, where the $n \times n$ matrix V_n is derived from the butterfly phylogeny assuming Brownian motion evolution, and the scalar σ_b^2 corresponds to the strength of phylogenetic signal. Random variable c_{ssp} gives the differences in mean Y across individual butterflies. Random variable d_{ssp} is similar to b_{ssp} but describes similarity in habitat use, with the expected covariance among species proportional to habitat overlap. Specifically, similarity in habitat use is estimated as the number of habitats shared among two species divided by the number of habitats used by the species with a narrower habitat range. The significance of fixed effects was tested using the z-scores of the coefficients. The significance of random effects was tested using a likelihood ratio test.

Mimetic Differences within Species. To test for flight mimicry over short evolutionary timescales, we also compared the flight of the comimetic Peruvian subspecies of *H. erato* (*H. e. emma* and *H. e. favorinus*) and *H. melpomene* (*H. m. aglaope* and *H. m. amaryllis*), which are parapatrically distributed dennis-rayed and postman subspecies of each species (79). WBF and wing angles were modeled separately against mimicry ring, species and sex, using a linear mixed-effects model implemented in the "lme4" package (80). Summary statistics were calculated using the "lmerTest" package (81). Data for each individual flight was used, and the individual was controlled for as a random effect.

Mimicry and Habitat. Comimetic species co-occur in part or across their entire distributions, making it difficult to establish the relative influences of mimicry and shared habitat on flight convergence. However, if flight convergence is driven more by mimicry than shared habitat, then the correlation between flight similarity and phylogenetic relatedness is expected to be weaker among mimetic co-occurring species compared to nonmimetic co-occurring species. This rationale was used to test for differences in ecological convergence in comimics and non-comimics in Elias et al. (82) and to test for evidence of selection in brain morphology divergence in Montgomery et al. (83). Using a Mantel test we compared the strength of this relationship in mimetic and nonmimetic species. Co-occurring species were defined as those sharing at least one common habitat type and region (see "Explanatory variables" methods and Dataset S1).

Using the data for all species, pairwise flight similarity distance matrices of WBF and wing angle means were built using the `dist()` function in R (84), and the phylogenetic distance matrix generated with the `cophenetic()` function from the `ape` package (85). From each of these matrices, we derived one matrix containing only pairwise values for co-occurring nonmimetic species and a second matrix containing only values for co-occurring mimetic species (all other values were replaced using NAs; Dataset S1). This allowed us to calculate correlation coefficients between pairwise flight similarity (WBF and both wing angles) and phylogenetic relatedness separately for the co-occurring mimetic and nonmimetic species.

The usual permutation-based Mantel test of the statistical significance of correlation between matrices is not valid when the matrices have a large proportion of null values. Instead, we derived the frequency distribution of correlation coefficients by generating 20,000 random phylogenetic trees, and for each created the same matrices for mimetic and nonmimetic co-occurring species as described above. This allowed us to calculate the probability of obtaining our observed correlation coefficients by chance using the function `pnorm()` in R.

Data, Materials, and Software Availability. All study data are included in the article and/or supporting information.

ACKNOWLEDGMENTS. This work was funded by Natural Environment Research Council (NERC) grant NE/K012886/1 to K.K.D., NERC Adapting to the Challenges of a Changing Environment Doctoral Training Partnership studentships to E.P. and L.M.Q., and Smithsonian Tropical Research Institute Short Term Fellowship to L.M.Q. We also thank Servicio Nacional Forestal y de Fauna Silvestre (SERFOR), the Peruvian Ministry of Agriculture, and the Area de Conservación Regional Cordillera Escalera for collecting permits (02 89-2014-MINAGRI-DGFFS/-DGEFFS, 020-014/GRSM/PEHCBM/DMA/ACR-CE, 040-2015/-GRSM/PEHCBM/DMA/ACR-CE). We are extremely grateful to

1. F. L. Condamine, M. E. Clapham, G. J. Kergoat, Global patterns of insect diversification: Towards a reconciliation of fossil and molecular evidence? *Sci. Rep.* **6**, 1–13 (2016).
2. K. E. Sears, R. R. Behringer, J. J. Rasweiler, L. A. Niswander, Development of bat flight: Morphologic and molecular evolution of bat wing digits. *Proc. Natl. Acad. Sci. U.S.A.* **103**, 6581–6586 (2006).
3. R. Dudley, Biomechanics of flight in neotropical butterflies: Morphometrics and kinematics. *J. Exp. Biol.* **150**, 37–53 (1990).
4. L. C. Johansson, P. Henningsson, Butterflies fly using efficient propulsive clap mechanism owing to flexible wings. *J. R. Soc. Interface* **18**, 20200854 (2021).
5. J. Prokop *et al.*, Paleozoic nymphal wing pads support dual model of insect wing origins. *Curr. Biol.* **27**, 263–269 (2017).
6. C. Le Roy, V. Debat, V. Llaurens, Adaptive evolution of butterfly wing shape: From morphology to behaviour. *Biol. Rev.* **94**, 1261–1281 (2019).
7. D. Outomuro *et al.*, Antagonistic natural and sexual selection on wing shape in a scrambling damselfly. *Evolution* **70**, 1582–1595 (2016).
8. D. L. Altshuler, R. Dudley, The physiology and biomechanics of avian flight at high altitude. *Integr. Comp. Biol.* **46**, 62–71 (2006).
9. M. K. Sridhar *et al.*, Effects of flight altitude on the lift generation of monarch butterflies: From sea level to overwintering mountain. *Bioinspir. Biomim.* **16**, 034002 (2021).
10. D. Kenna, S. Pawar, R. J. Gill, Thermal flight performance reveals impact of warming on bumblebee foraging potential. *Funct. Ecol.* **35**, 2508–2522 (2021), 10.1111/1365-2435.13887.
11. D. L. Altshuler, R. Dudley, J. A. McGuire, Resolution of a paradox: Hummingbird flight at high elevation does not come without a cost. *Proc. Natl. Acad. Sci. U.S.A.* **101**, 17731–17736 (2004).
12. L. J. Dällenbach, A. Glauser, K. S. Lim, J. W. Chapman, M. H. M. Menz, Higher flight activity in the offspring of migrants compared to residents in a migratory insect. *Proc. R. Soc. B* **285**, 20172829 (2018).
13. L. Chittka, A. Gumbert, J. Kunze, Foraging dynamics of bumble bees: Correlates of movements within and between plant species. *Behav. Ecol.* **8**, 239–249 (1997).
14. P. J. DeVries, C. M. Penz, R. I. Hill, Vertical distribution, flight behaviour and evolution of wing morphology in Morpho butterflies. *J. Anim. Ecol.* **79**, 1077–1085 (2010).
15. A. O. Ancel *et al.*, Aerodynamic evaluation of wing shape and wing orientation in four butterfly species using numerical simulations and a low-speed wind tunnel, and its implications for the design of flying micro-robots. *Interface Focus* **7**, 20160087 (2017).
16. C. Le Roy *et al.*, Convergent morphology and divergent phenology promote the coexistence of *Morpho* butterfly species. *Nat. Commun.* **12**, 1–9 (2021).
17. A. C. V. Balogh, G. Gamberale-Stille, O. Leimar, Learning and the mimicry spectrum: From quasi-Bates to super-Müller. *Anim. Behav.* **76**, 1591–1599 (2008).
18. H. W. Bates, Contributions to an insect fauna of the Amazon Valley. Lepidoptera: Heliconiidae. *Trans. Linn. Soc. Lond.* **23**, 495–566 (1862).
19. F. Müller, Ituna and Thyridia: A remarkable case of mimicry in butterflies. *Trans. Entomol. Soc. Lond.* **91**, 100 (1879).
20. D. W. Kikuchi, D. W. Pfennig, Predator cognition permits imperfect coral snake mimicry. *Am. Nat.* **176**, 830–834 (2010).
21. A. Amézquita *et al.*, Conspicuousness, color resemblance, and toxicity in geographically diverging mimicry: The pan-Amazonian frog *Allobates femoralis*. *Evolution* **71**, 1039–1050 (2017).
22. K. R. Willmott, M. Elias, A. Sourakov, Two possible caterpillar mimicry complexes in Neotropical danaïde butterflies (Lepidoptera: Nymphalidae). *Ann. Entomol. Soc. Am.* **104**, 1108–1118 (2011).
23. J. N. Huang, R. C. Cheng, D. Li, I. M. Tso, Salticid predation as one potential driving force of ant mimicry in jumping spiders. *Proc. R. Soc. B: Biol. Sci.* **278**, 1356 (2011).
24. T. Kitamura, M. Imafuku, Behavioural mimicry in flight path of Batesian intraspecific polymorphic butterfly *Papilio polytes*. *Proc. R. Soc. B: Biol. Sci.* **282**, 20150483 (2015).
25. M. A. Skowron Volponi, D. J. McLean, P. Volponi, R. Dudley, Moving like a model: Mimicry of hymenopteran flight trajectories by clearingwing moths of Southeast Asian rainforests. *Biol. Lett.* **14**, 20180152 (2018).
26. R. B. Srygley, Locomotor mimicry in *Heliconius* butterflies: Contrast analyses of flight morphology and kinematics. *Philos. Trans. R. Soc. Lond. B: Biol. Sci.* **354**, 203–214 (1999).
27. R. M. Merrill *et al.*, The diversification of *Heliconius* butterflies: What have we learned in 150 years? *J. Evol. Biol.* **28**, 1417–1438 (2015).
28. K. M. Kozak *et al.*, Multilocus species trees show the recent adaptive radiation of the mimetic *Heliconius* butterflies. *Syst. Biol.* **64**, 505–524 (2015).
29. M. Arias *et al.*, Variation in cyanogenic compounds concentration within a *Heliconius* butterfly community: Does mimicry explain everything? *BMC Evol. Biol.* **16**, 1–10 (2016).
30. M. Chouteau, M. Arias, M. Joron, Warning signals are under positive frequency dependent selection in nature. *Proc. Natl. Acad. Sci. U.S.A.* **113**, 2164–2169 (2016).
31. D. D. Dell'Aglio, J. Troscianko, W. O. McMillan, M. Stevens, C. D. Jiggins, The appearance of mimetic *Heliconius* butterflies to predators and conspecifics. *Evolution* **72**, 2156–2166 (2018).
32. J. Mallet, L. E. Gilbert, Why are there so many mimicry rings? Correlations between habitat, behaviour and mimicry in *Heliconius* butterflies. *Biol. J. Linn. Soc.* **55**, 159–180 (1995).
33. J. R. G. Turner, Adaptation and evolution in *Heliconius*: A defense of NeoDarwinism. *Annu. Rev. Ecol. Syst.* **12**, 99–121 (1981).
34. G. Beccaloni, Ecology, natural history and behaviour of Ithomiine butterflies and their mimics in Ecuador (Lepidoptera: Nymphalidae: Ithomiinae). *Trop. Lepidoptera* **8**, 103–124 (1997).
35. K. S. Brown, Adult-obtained pyrrolizidine alkaloids defend ithomiine butterflies against a spider predator. *Nature* **309**, 707–709 (1984).
36. R. T. Jones *et al.*, Wing shape variation associated with mimicry in butterflies. *Evolution* **67**, 2323–2334 (2013).
37. C. Mérot, Y. Le Poul, M. Théry, M. Joron, Refining mimicry: Phenotypic variation tracks the local optimum. *J. Anim. Ecol.* **85**, 1056–1069 (2016).
38. D. O. Rossato *et al.*, Subtle variation in size and shape of the whole forewing and the red band among co-mimics revealed by geometric morphometric analysis in *Heliconius* butterflies. *Ecol. Evol.* **8**, 3280–3295 (2018).
39. R. I. Hill, Convergent flight morphology among Müllerian mimic mutualists. *Evolution* **75**, 2460–2479 (2021).
40. K. S. Brown, The biology of *Heliconius* and related genera. *Annu. Rev. Entomol.* **26**, 427–457 (1981).
41. G. Montejo-Kovacevich *et al.*, Altitude and life-history shape the evolution of *Heliconius* wings. *Evolution* **73**, 2436–2450 (2019).
42. M. Joron, Polymorphic mimicry, microhabitat use, and sex-specific behaviour. *J. Evol. Biol.* **18**, 547–556 (2005).
43. S. Mena, K. M. Kozak, R. E. Cárdenas, M. F. Checa, Forest stratification shapes allometry and flight morphology of tropical butterflies. *Proc. Biol. Sci.* **287**, 20201071 (2020).
44. S. M. Van Belleghem *et al.*, Selection and isolation define a heterogeneous divergence landscape between hybridizing *Heliconius* butterflies. *Evolution* **75**, 2251–2268 (2021).
45. A. Y. Kawahara *et al.*, Phylogenomics reveals the evolutionary timing and pattern of butterflies and moths. *Proc. Natl. Acad. Sci. U.S.A.* **116**, 22657–22663 (2019).
46. J. P. Dumbacher, R. C. Fleischer, Phylogenetic evidence for colour pattern convergence in toxic pitohuis: Müllerian mimicry in birds? *Proc. R. Soc. Lond. B Biol. Sci.* **268**, 1971–1976 (2001).
47. E. Twomey *et al.*, Mechanisms for color convergence in a mimetic radiation of poison frogs. *Am. Nat.* **195**, E132–E149 (2020).
48. F. Schiestl *et al.*, Sex pheromone mimicry in the early spider orchid (*Ophrys sphegodes*): Patterns of hydrocarbons as the key mechanism for pollination by sexual deception. *J. Comp. Physiol. A* **186**, 567–574 (2000).
49. H. D. Penney, C. Hassall, J. H. Skevington, B. Lamborn, T. N. Sherratt, The relationship between morphological and behavioral mimicry in hover flies (Diptera: Syrphidae). *Am. Nat.* **183**, 281–289 (2015), 10.1086/674612.
50. M. McClure *et al.*, Why has transparency evolved in aposomatic butterflies? Insights from the largest radiation of aposomatic butterflies, the Ithomiini. *Proc. R. Soc. B: Biol. Sci.* **286**, 20182769 (2019).
51. K. S. Brown, W. W. Benson, Adaptive polymorphism associated with multiple mullerian mimicry in *Heliconius numata* (Lepid. Nymph.). *Biotropica* **6**, 205–228 (1974).
52. K. R. Willmott, A. V. L. Freitas, Higher-level phylogeny of the Ithomiinae (Lepidoptera: Nymphalidae): Classification, patterns of larval hostplant colonization and diversification. *Cladistics* **22**, 297–368 (2006).
53. J. R. Trigo *et al.*, Pyrrolizidine alkaloids: Different acquisition and use patterns in Apocynaceae and Solanaceae feeding ithomiine butterflies (Lepidoptera: Nymphalidae). *Biol. J. Linn. Soc.* **58**, 99–123 (1996).
54. S. H. Montgomery, R. M. Merrill, S. R. Ott, Brain composition in *Heliconius* butterflies, posteclosion growth and experience-dependent neuropil plasticity. *J. Comp. Neurol.* **524**, 1747–1769 (2016).
55. B. J. Morris, A. Couto, A. Aydin, S. H. Montgomery, Re-emergence and diversification of a specialized antennal lobe morphology in ithomiine butterflies. *Evolution* **75**, 3191–3202 (2021), 10.1111/EVO.14324.

Author affiliations: ^aDepartment of Biology, University of York, Heslington YO10 5DD, United Kingdom; ^bDivision of Evolutionary Biology, Ludwig-Maximilians-Universität München, Planegg-Martinsried 82152, Germany; ^cDepartment of Organismic and Evolutionary Biology, Harvard University, Cambridge, MA 02138; ^dEcology and Evolutionary Biology, School of Biosciences, The University of Sheffield, Sheffield S10 2TN, United Kingdom; ^eTree of Life Programme, Wellcome Sanger Institute, Hinxton, Cambridge CB10 1SA, United Kingdom; ^fSmithsonian Tropical Research Institute, Apartado, Panamá 0843-03092, Republic of Panama; and ^gPest Management Research Unit, Agricultural Research Service, United States Department of Agriculture, Sidney, MT 59270

56. F. Mann *et al.*, The scent chemistry of *Heliconius* wing androconia. *J. Chem. Ecol.* **43**, 843–857 (2017).
57. S. Schulz *et al.*, Semiochemicals derived from pyrrolizidine alkaloids in male ithomiine butterflies (Lepidoptera: Nymphalidae: Ithomiinae). *Biochem. Syst. Ecol.* **32**, 699–713 (2004).
58. H. Schmaljohann, F. Liechti, Adjustments of wingbeat frequency and air speed to air density in free-flying migratory birds. *J. Exp. Biol.* **212**, 3633–3642 (2009).
59. M. E. Dillon, M. R. Frazier, *Drosophila melanogaster* locomotion in cold thin air. *J. Exp. Biol.* **209**, 364–371 (2006).
60. M. P. T. G. Tercel, F. Veronesi, T. W. Pope, Phylogenetic clustering of wingbeat frequency and flight-associated morphometrics across insect orders. *Physiol. Entomol.* **43**, 149–157 (2018).
61. R. W. R. Wallbank *et al.*, Evolutionary novelty in a butterfly wing pattern through enhancer shuffling. *PLoS Biol.* **14**, e1002353 (2016).
62. S. M. Van Belleghem *et al.*, Complex modular architecture around a simple toolkit of wing pattern genes. *Nat. Ecol. Evol.* **1**, 1–12 (2017).
63. S. H. Martin *et al.*, Genome-wide evidence for speciation with gene flow in *Heliconius* butterflies. *Genome Res.* **23**, 1817–1828 (2013).
64. N. Rosser, *et al.*, Hybrid speciation driven by multilocus introgression of ecological traits. *Nature*, in press.
65. R. B. Srygley, Locomotor mimicry in butterflies? The associations of positions of centres of mass among groups of mimetic, unprofitable prey. *Philos. Trans. R. Soc. B: Biol. Sci.* **343**, 145–155 (1994).
66. R. B. Srygley, P. Chai, Flight morphology of Neotropical butterflies: Palatability and distribution of mass to the thorax and abdomen. *Oecologia* **84**, 491–499 (1990).
67. N. Rosser *et al.*, Geographic contrasts between pre- and postzygotic barriers are consistent with reinforcement in *Heliconius* butterflies. *Evolution* **73**, 1821–1838 (2019).
68. R. B. Srygley, Evolution of the wave: Aerodynamic and aposematic functions of butterfly wing motion. *Proc. R. Soc. B: Biol. Sci.* **274**, 913–917 (2007).
69. C. T. Rueden *et al.*, ImageJ2: ImageJ for the next generation of scientific image data. *BMC Bioinformatics* **18**, 529 (2017).
70. N. Rosser, K. M. Kozak, A. B. Phillimore, J. Mallet, Extensive range overlap between heliconiine sister species: Evidence for sympatric speciation in butterflies? *BMC Evol. Biol.* **15**, 1–13 (2015).
71. L. C. Evans *et al.*, The importance of including habitat-specific behaviour in models of butterfly movement. *Oecologia* **193**, 249–259 (2020).
72. P. J. DeVries, *The butterflies of Costa Rica and their natural history. Volume I: Papilionidae, Pieridae, Nymphalidae*. (Princeton University Press, 1987).
73. C. D. Jiggins, W. O. McMillan, W. Neukirchen, J. Mallet, What can hybrid zones tell us about speciation? The case of *Heliconius erato* and *H. himera* (Lepidoptera: Nymphalidae). *Biol. J. Linn. Soc.* **59**, 221–242 (1996).
74. J. G. Kingsolver, Experimental analyses of wing size, flight, and survival in the western white butterfly. *Evolution* **53**, 1479–1490 (1999).
75. S.-P. Quek *et al.*, Dissecting comimetic radiations in *Heliconius* reveals divergent histories of convergent butterflies. *Proc. Natl. Acad. Sci. U.S.A.* **107**, 7365 (2010).
76. H. M. Hines *et al.*, Wing patterning gene redefines the mimetic history of *Heliconius* butterflies. *Proc. Natl. Acad. Sci. U.S.A.* **108**, 19666–19671 (2011).
77. A. R. Ives, M. R. Helmus, Generalized linear mixed models for phylogenetic analyses of community structure. *Ecol. Monogr.* **81**, 511–525 (2011).
78. D. Li, A. R. Ives, D. M. Waller, Can functional traits account for phylogenetic signal in community composition? *New Phytol.* **214**, 607–618 (2017).
79. N. Rosser, K. K. Dasmahapatra, J. Mallet, Stable *Heliconius* butterfly hybrid zones are correlated with a local rainfall peak at the edge of the Amazon basin. *Evolution* **68**, 3470–3484 (2014).
80. D. Bates, M. Mächler, B. M. Bolker, S. C. Walker, Fitting linear mixed-effects models using lme4. *J. Stat. Softw.* **67**, 1–48 (2015).
81. A. Kuznetsova, P. B. Brockhoff, R. H. B. Christensen, lmerTest package: Tests in linear mixed effects models. *J. Stat. Softw.* **82**, 1–26 (2017).
82. M. Elias, Z. Gompert, C. Jiggins, K. Willmott, Mutualistic interactions drive ecological niche convergence in a diverse butterfly community. *PLoS Biol.* **6**, e300 (2008).
83. S. H. Montgomery, M. Rossi, W. O. McMillan, R. M. Merrill, Neural divergence and hybrid disruption between ecologically isolated *Heliconius* butterflies. *Proc. Natl. Acad. Sci. U.S.A.* **118**, 2021 (2021).
84. R Core Team, *R: A Language and Environment for Statistical Computing* (R Foundation for Statistical Computing, 2018).
85. E. Paradis, K. Schliep, An environment for modern phylogenetics and evolutionary analyses in R. *Bioinformatics* **35**, 526–528 (2019).